Research Article | Vol. 25, No. 4 | 20 Feb 2017 | OPTICS EXPRESS 3795

Optics EXPRESS

Combination of micro-scanning mirrors and multi-mode fibers for speckle reduction in high lumen laser projector applications

ZHAOMIN TONG,[1,2,*] WENJIANG SHEN,[3] SHAOHUA SONG,[1,2] WENZHI CHENG,[1,2] ZHUO CAI,[1,2] YIFEI MA,[1,2] LEI WEI,[4] WEIGUANG MA,[1,2] LIANTUAN XIAO,[1,2] SUOTANG JIA,[1,2] AND XUYUAN CHEN,[1,2,5,6]

[1]*State Key Laboratory of Quantum Optics and Quantum Optics Devices, Institute of Laser Spectroscopy, Shanxi University, Taiyuan, Shanxi 030006, China*
[2]*Collaborative Innovation Center of Extreme Optics, Shanxi University, Taiyuan, Shanxi 030006, China*
[3]*Suzhou Institute of Nano-Tech and Nano-Bionics, Chinese Academy of Science, Suzhou, Jiangsu 215123, China*
[4]*School of Electrical and Electronic Engineering, Nanyang Technological University, Singapore 639798, Singapore*
[5]*Faculty of Technology and Maritime Sciences, Department of Micro- and Nanosystem Technology, University College of Southeast Norway, Borre N-3184, Norway*
[6]*xuyuan.chen@usn.no*
[*]*zhaomin.tong@sxu.edu.cn*

Abstract: In high lumen laser projectors, it is required to use laser diodes coupled to multi-mode fibers (MMFs) to obtain a high power illumination module. In this paper, we have fabricated an electromagnetic micro-scanning mirror (EM-MSM), and we have firstly demonstrated a speckle reduction method by the combination of the EM-MSM and the MMF. With the help of a condenser lens, laser beams modulated and reflected from the EM-MSM are coupled into the MMF within its acceptance angle. Because the fast scanning behavior of the EM-MSM results in the phase modulation and mode coupling among the MMF guided modes, the light intensity field distributions at the exit aperture of the MMF are changing. During the charge-coupled device (CCD) integration time, the random speckle patterns are integrated and homogenized by the CCD camera, and hence speckle is reduced. By driving the EM-MSM in raster scan, the lowest compound speckle contrast ratio at 0.0794 is obtained, where the EM-MSM half scanning angles are 0.4 ° and the optical power loss is lower than 4.5%. The demonstrated technique is compact and can endure the high power of the laser module; thus, it has a promising potential in high lumen laser projector applications.

OCIS codes: (030.1640) Coherence; (030.6140) Speckle; (120.2040) Displays.

References and links

1. M. S. Brennesholtz and E. H. Stupp, *Projection Displays* (John Wiley & Sons Ltd, 2008).
2. L. Jiang, J. Liu, A. Tian, Y. Cheng, Z. Li, L. Zhang, S. Zhang, D. Li, M. Ikeda, and H. Yang, "GaN-based green laser diodes," J. Semicond. **37**(11), 111001 (2016).
3. J. W. Goodman, *Speckle Phenomena in Optics: Theory and Applications* (Roberts and Company Publishers, 2006).
4. A. Furukawa, N. Ohse, Y. Sato, D. Imanishi, K. Wakabayashi, S. Ito, K. Tamamura, and S. Hirata, "Effective speckle reduction in laser projection displays," Proc. SPIE **6911**, 69110T (2008).
5. C. Saloma, S. Kawata, and S. Minami, "Speckle reduction by wavelength and space diversity using a semiconductor laser," Appl. Opt. **29**(6), 741–742 (1990).
6. S. C. Shin, S. S. Yoo, S. Y. Lee, C. Park, S. Park, J. W. Kwon, and S. Lee, "Removal of hot spot speckle on laser projection screen using both the running screen and the rotating diffuser," J. Disp. Technol. **27**(3), 91–96 (2006).
7. S. Kubota and J. W. Goodman, "Very efficient speckle contrast reduction realized by moving diffuser device," Appl. Opt. **49**(23), 4385–4391 (2010).
8. J. I. Trisnadi, "Hadamard speckle contrast reduction," Opt. Lett. **29**(1), 11–13 (2004).
9. M. N. Akram, V. Kartashov, and Z. Tong, "Speckle reduction in line-scan laser projectors using binary phase codes," Opt. Lett. **35**(3), 444–446 (2010).

#284020 https://doi.org/10.1364/OE.25.003795
Journal © 2017 Received 4 Jan 2017; revised 3 Feb 2017; accepted 3 Feb 2017; published 13 Feb 2017

Optics EXPRESS

10. Z. Tong, M. N. Akram, and X. Chen, "Speckle reduction using orthogonal arrays in laser projectors," Appl. Opt. **49**(33), 6425–6429 (2010).
11. Z. Tong and X. Chen, "Principle, design and fabrication of a passive binary micro-mirror array (BMMA) for speckle reduction in Grating Light Valve (GLV) based laser projection display," Sensor. Actuat. A-Phys. **210**, 209–216 (2014).
12. Z. Tong and X. Chen, "A ferroelectric liquid crystal spatial light modulator encoded with orthogonal arrays and its optimized design for laser speckle reduction," Opt. Lasers Eng. **90**, 173–178 (2017).
13. B. Silverstein, A. Kurtz, J. Bietry, and G. Northhard, "A laser beased digital cinema projector," Soc. Inf. Disp. Int. Symp. Dig. Tech. Pap. **42**, 326–329 (2011).
14. Z. Tong and X. Chen, "Speckle contrast for superposed speckle patterns created by rotating the orientation of laser polarization," J. Opt. Soc. Am. A **29**(10), 2074–2079 (2012).
15. M. N. Akram, Z. Tong, G. Ouyang, X. Chen, and V. Kartashov, "Laser speckle reduction due to spatial and angular diversity introduced by fast scanning micromirror," Appl. Opt. **49**(17), 3297–3304 (2010).
16. Z. Tong, X. Chen, M. N. Akram, and A. Aksnes, "Compound speckle characterization method and reduction by optical design," J. Disp. Technol. **8**(3), 132–137 (2012).
17. W. Ha, S. Lee, Y. Jung, J. Kim, and K. Oh, "Speckle reduction in multimode fiber with a piezoelectric transducer in radial vibration for fiber laser marking and display applications," Proc. SPIE **6873**, 68731V (2008).
18. W. Ha, S. Lee, Y. Jung, J. K. Kim, and K. Oh, "Acousto-optic control of speckle contrast in multimode fibers with a cylindrical piezoelectric transducer oscillating in the radial direction," Opt. Express **17**(20), 17536–17546 (2009).
19. D. S. Mehta, D. N. Naik, R. K. Singh, and M. Takeda, "Laser speckle reduction by multimode optical fiber bundle with combined temporal, spatial, and angular diversity," Appl. Opt. **51**(12), 1894–1904 (2012).
20. Y. Fujimaki and H. Taniguchi, "Reduction of speckle contrast in multimode fibers using piezoelectric vibrator," Proc. SPIE **8960**, 89601S (2014).
21. J. Kinoshita, H. Aizawa, A. Takamori, K. Yamamoto, H. Murata, and K. Tojo, "Angular dependence of screen speckle and fiber speckle of coupled output of nine high-power blue laser diodes through a multi-mode fiber," Opt. Rev. **23**(1), 121–132 (2016).
22. G. Zheng, B. Wang, T. Fang, H. Cheng, Y. Qi, Y. W. Wang, B. X. Yan, Y. Bi, Y. Wang, S. W. Chu, T. J. Wu, J. K. Xu, H. T. Min, S. P. Yan, C. W. Ye, and Z. D. Jia, "Laser digital cinema projector," J. Disp. Technol. **4**(3), 314–318 (2008).
23. J. He, P. Zhou, H. Yu, J. Shen, and J. Si, "Research on large size MEMS scanning mirror driven by electromagnetic," Acta Phtonica Sin. **46**(1), 0123003 (2017).
24. P. J. Kajenski, P. L. Fuhr, and D. R. Huston, "Mode coupling and phase modulation in vibrating waveguides," J. Lightwave Technol. **10**(9), 1297–1301 (1992).
25. P. Hlubina, "Spectral and dispersion analysis of laser sources and multimode fibres via the statistics of the intensity pattern," J. Mod. Opt. **41**(5), 1001–1014 (1994).
26. B. E. A. Saleh and M. C. Teich, *Fundamentals of Photonics* (John Wiley & Sons Inc., 2009)
27. S. Roelandt, Y. Meuret, G. Craggs, G. Verschaffelt, P. Janssens, and H. Thienpont, "Standardized speckle measurement method matched to human speckle perception in laser projection systems," Opt. Express **20**(8), 8770–8783 (2012).

1. Introduction

In projection displays, comparing to the illumination by lamps, solid-state light sources including solid-state lasers and light emitting diodes (LEDs) can provide wider color gamut and longer lifetime *etc*. The LED technology, however, is not bright enough for high lumen projection displays, where its typical brightness is limited to about 2000 lumen [1]; laser diodes are the potential candidate for mass production in high lumen projection displays, but they currently face the problems of the high cost of green color and speckle [2,3]. With the development of gallium nitride-based materials, the price of green laser diodes is expected to reduce in the next few years [2].

Speckle as the disturbance in laser projection displays can greatly affect the image quality, and hence it must be suppressed. In general, speckle reduction can be achieved by spectrum widened lasers [4], by wavelength diversity [5], by fast vibrating or rotating the screen [6], by projecting a fast changing random diffuser or a fast changing binary diffuser with predetermined phase distributions onto the screen [7–12], by using other time varying components [13], by polarization diversity [13, 14], or by angle diversity [13, 15, 16], *etc*. In purpose to reduce speckle more efficiently, people also compound different speckle reduction techniques. If there are n independent speckle reduction mechanisms, and the ith speckle reduction technique can provide N_i degrees of speckle reduction freedom, after compounding these speckle reduction techniques, the speckle contrast ratio C (CR, defined as the ratio

Optics EXPRESS

between the standard deviation and the mean value of the light intensity) can be reduced from one to [3]

$$C = \frac{1}{\sqrt{\prod_{i=1}^{n} N_i}}. \quad (1)$$

Vibrating multi-mode fibers (MMFs) using vibrator or cylindrical piezoelectric transducer is another research direction for speckle reduction [17–21]. The inherent merits of this method are: firstly, currently coupling the outputs of laser diodes into the corresponding MMFs to achieve a high power illumination module is cost effective solution in high lumen laser projectors, and secondly, this technique is a remote method which is not within the projectors, *i.e.*, the projection system can be kept as it is [21, 22]. The speckle reduction mechanism of this method is the modulation of light distributions at the exit aperture of the MMF due to the phase modulation and mode coupling among the guided modes. When the exposure time of the detector (for example, the charge-coupled device: CCD camera) is longer than the MMFs modulation cycle, different speckle patterns are integrated and homogenized. Therefore, the summed speckle image has a lower speckle CR, and speckle reduction is achieved.

As the driver to vibrate the MMF, vibrators and cylindrical piezoelectric transducers are bulky [17–21]. In our previous publications, we have introduced an electrostatic micro-scanning mirror (MSM) by employing the spatial and angular diversity for speckle reduction [15, 16]. This method, however, cannot endure the high power lasers in high lumen projection displays due to the small size of the reflecting mirror. The tens watt optical power of the laser module can cause unstable working condition of the MSM by heat accumulation or even burn the MSM after long-time illuminations. In this paper, we firstly propose the speckle reduction in high lumen laser projection displays by the combination of an electromagnetic MSM (EM-MSM) and the MMF. Instead of vibrating the MMF, the dynamic light distributions at the exit aperture of the MMF is obtained by the scanning behavior of the EM-MSM, where the EM-MSM reflects different laser beams into the entrance aperture of the MMF. We have experimentally demonstrated the speckle reduction efficiency by the combination of the EM-MSM and the MMF, and we have discussed its potential application in high lumen laser projection displays. This method is compact and it can endure the high power laser module, where laser beams generated by laser diodes are modulated by the corresponding MSMs; thus, it has a promising potential in high lumen laser projector applications.

2. EM-MSM fabrications and characterizations

Among electrostatic, piezoelectric, electro-thermal, and electromagnetic MSMs, the EM-MSM has the merits of large scanning angles under low driving voltage and good linearity [23]. Figure 1(a) schematically shows the working principle of the EM-MSM for horizontal scan. A pair of electromagnetic coils is placed underneath the MSM, where a ring-type permanent magnet is glued to the backside of the MSM. By sending complementary driving signals to the electromagnetic coils, they work in push-pull action, and horizontal scan can be achieved. Similarly, vertical scan can be obtained by placing another pair of electromagnetic coils orthogonally to the first pair; thus, after using two pairs of electromagnetic coils, raster scan is obtained [23].

Fabrication process of the EM-MSM starts from the deposition of a 10 nm thick titanium (Ti) layer on the backside of a 350 μm thick double-sides polished n-type (100) silicon wafer by magnetron sputtering, followed by the deposition of a 300 nm thick copper (Cu) layer also by magnetron sputtering. The Ti/Cu thin films work as the protection layers for the backside silicon from the following silicon etch process. Photoresist is spin-coated, exposed and removed by lithography process on the front side of the silicon wafer, and the 350 μm thick silicon wafer is etched thoroughly by deep reactive ion etch with tetrafluoromethane,

Optics EXPRESS

octafluorocyclobutane and oxygen mixtures. Later, the front side photoresist layer and backside Ti/Cu protection layer are removed, and we evaporate a thin gold film as the reflection layer on the front side. As the final step, the micro mirror die is separated and packaged by gluing a ring-type rubidium iron boron magnet on the die backside, where the diameter of the interior circular mirror is 13 mm. Figure 1(b) shows the packaged EM-MSM [23].

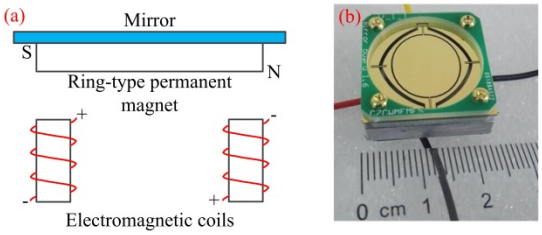

Fig. 1. (a) Working principle of the EM-MSM for horizontal scan and (b) the packaged EM-MSM after fabrication.

The resistance of the EM-MSM is measured equaling to 19.1 Ω. Figure 2 shows the relationship between the driving voltage (peak to peak) and the half scanning angle of the EM-MSM θ_m. In Fig. 2, the EM-MSM has two scanning directions driven independently by function generators. Sinusoidal waveforms are used, where the driving frequencies are f_h = 348 Hz for the horizontal scan and f_v = 660 Hz for the vertical scan. The scanning angles of the EM-MSM are adjusted by setting the peak to peak voltages ranging from 60 mV to 1 V for the horizontal scan and from 30 mV to 930 mV for the vertical scan, respectively.

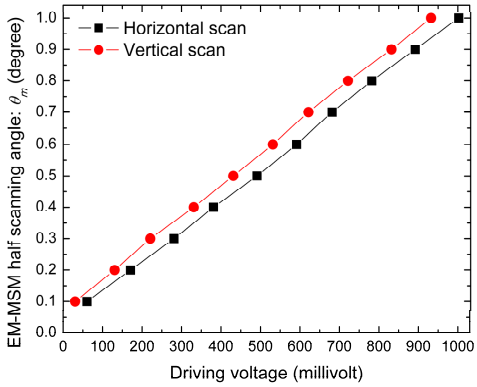

Fig. 2. The relationship between the peak to peak driving voltage and the EM-MSM half scanning angle θ_m.

3. Speckle reduction theory and experiments

3.1 Theory

The number of modes M for step-index MMFs can be expressed as

$$M = \frac{16a^2\left(n_1^2 - n_2^2\right)}{\lambda^2}, \tag{2}$$

where λ, a, n_1 and n_2 represent the wavelength of coupled light, the core radius, and the refractive index of the core and cladding, respectively.

When a coherent laser beam is coupled into the MMF, speckle forms at the exit aperture of the MMF due to the phase delays among different guided fiber modes and the light interference. External disturbances like vibrating the MMF or changing the angle of incidence

Optics EXPRESS

of the coupled laser beam temporally vary the optical power of the modes. Power change of the kth guided mode $\triangle P_k$ can be written as [24]

$$\Delta P_k = \sum_{l=1}^{L} h_{k,l}\left(P_k - P_l\right), \tag{3}$$

where P_k and P_l are the powers in guided modes k and l, respectively, $h_{k,l}$ is the coupling coefficient between the guided modes k and l, and the value of k and l is less than m (m is the number of guided modes, $m \le M$). Under external disturbances, the coupling coefficient $h_{k,l}$ between the guided modes k and l changes randomly, and consequently the random phase variations resulted from the phase delays between the m guided modes are uniformly and independently distributed on the interval $[0, 2\pi]$. By assuming that the optical powers of the guided modes are equal, and if the value of m is large, the speckle CR at the exit aperture of the MMF C_f can be written as

$$C_f = \frac{1}{m\Delta\tau}\sqrt{\int_0^{m\Delta\tau} 2\left(m\Delta\tau - \tau\right)\left|\gamma(\tau)\right| d\tau}, \tag{4}$$

where τ, $\triangle\tau$ and γ represent the delay time of the guided modes, the delay time difference between the kth and the (k-1)th guided modes, and the complex degree of temporal coherence of the laser source field, respectively [25].

According to Eq. (4), the speckle CR C_f is inverse proportional to the value of m. Therefore, by temporally changing the angle of incidence of the coupled laser beam, such as by introducing the scanning behavior using the EM-MSM, speckle reduction can be obtained at the exit aperture of the MMF; for larger scanning angle, the value of m is increasing, and we can achieve a more efficient speckle reduction.

3.2 Experiments

Figure 3 shows the experimental setup. A collimated 50 mW green laser diode at wavelength λ = 520 nm illuminates the EM-MSM which reflects the collimated laser beam along different directions. Diameters of the collimated laser beam are measured as 0.6 mm along the horizontal direction and 0.7 mm along the vertical direction. A temperature-controlled mount has been used to maintain the laser diode working temperature at a constant level of 15 °C. Before this experiment, we have characterized the coherence property of the laser diode, where the speckle contrast CR is measured equaling to 0.71 in free space by directly illuminating the laser diode to a sandblasted glass. By introducing a condenser lens of 60 mm focal length, the modulated laser beams are coupled into the MMF. Diameter of the condenser lens should be large enough to fully collect the modulated laser beams, *i.e.*, to avoid any extra optical power loss when the EM-MSM is scanning. The condenser lens used here has a diameter at 50.8 mm, which is sufficient to collect all the modulated laser beams. Distances between the EM-MSM and the condenser lens and between the condenser lens and the MMF are 360 mm and 72 mm, respectively. Refractive indexes of the core and the cladding of the MMF equal to n_1 = 1.492 and n_2 = 1.402, and the radius of the core is a = 1.47 mm. A 5 mm × 5 mm highly transparent diffuser (manufactured by using fused silica material, transmission >98% for visible light by double side anti-reflective coating, and half scattering angles at about 2 degree in both horizontal and vertical directions) is placed before the entrance aperture (size: 3.5 mm × 3.5 mm) of a 140 mm long tapered rod integrator to enhance the homogenizing effect of the tapered rod integrator. An f_p = 25.4 mm focal length and D_p = 25.4 mm diameter projection lens projects the exit aperture (size: 8.16 mm × 4.74 mm) of the tapered rod integrator onto the screen (white Lambertian surface, screen gain at 1). For the same optical power loss consideration as the condenser lens, and because the etendue of optical system increases when the EM-MSM is scanning, diameter of the projection lens should also be large enough. In our experiment, we have observed that the optical field is always within the projection lens pupil. Distances between the exit aperture of the tapered rod

Optics EXPRESS

integrator and the projection lens and between the projection lens and the screen are 260 mm and Z_p = 1025 mm, respectively. We have used a CCD camera with 1280 × 1024 pixels to capture the speckle images (pixel width 5.2 μm), and the imaging lens mounted on the CCD camera has a focal length at f_i = 35 mm.

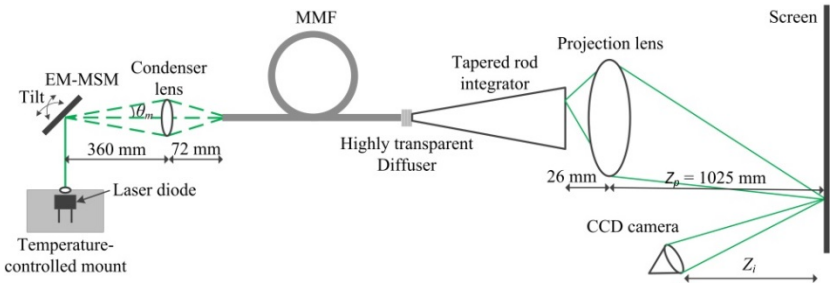

Fig. 3. Experimental setup. The collimated laser beam is modulated by the electromagnetic micro scanning mirror: EM-MSM, and with the help of the condenser lens, it is coupled into the multi-mode fiber: MMF. The highly transparent diffuser and the tapered rod integrator together homogenize the optical field. The exit aperture of the tapered rod integrator is projected onto the screen by the projection lens, and the speckle image is captured by the CCD camera mounted with an imaging lens.

Assume that one EM-MSM scanning cycle can generate T independent speckle images (T is the temporal degree of speckle reduction freedom), exposure time of the CCD camera should not be shorter than one EM-MSM scanning cycle to integrate all these T independent speckle images. According to Eq. (1), speckle can be reduced by $1/T^{1/2}$. Also, because the scanning routes for the EM-MSM during its different scanning cycles are identical, these T independent speckle images are repeated, *i.e.*, they are totally dependent; thus, speckle will not be reduced further by increasing the number of scanning cycles during the CCD camera integration time [3,15]. In our experiments, to capture and integrate all the T independent speckle images during at least one EM-MSM scanning cycle, we set the exposure time of the CCD camera as 30 ms. The experiments are conducted in a dark room on top of an optical table to avoid the disturbances from background lights and environmental vibrations; thus, we make sure that the speckle images captured by the CCD camera are correct.

4. Results and discussions

4.1 Optical power loss

Currently, due to the high cost of green color, optical power loss is a main concern when we reduce speckle, where it should be suppressed as low as possible [1,2]. The total internal reflection condition of the MMF requires that the largest angle of incidence of the coupled laser beams should not be larger than the acceptance angle of the MMF θ_a. The expression to calculate θ_a can be written as [26]

$$\theta_a = \sin^{-1}\left(\sqrt{n_1^2 - n_2^2}\right), \tag{5}$$

which equals to 30.7 ° after substituting n_1 = 1.492 and n_2 = 1.402. In our experiment, the largest horizontal and vertical half scanning angles of the EM-MSM are 1 °, which correspond to the largest half angles of incidence of the coupled laser beams along the horizontal and vertical directions equal to 5 ° after the five times magnification by the condenser lens. Under this circumstance, we can make sure that the coupled lights are all guided within the MMF.

The optical power loss is measured by an optical power meter which is placed closely after the exit aperture of the MMF. Figure 4 shows the relationship between the EM-MSM half scanning angle θ_m and the optical power loss (defined as the optical power ratio when the

Optics EXPRESS

EM-MSM is turned on and turned off). We can find that with the increment of the value of θ_m, the optical power loss also increases; while when $\theta_m \leq 0.4$ °, lower than 4.5% optical power losses are obtained.

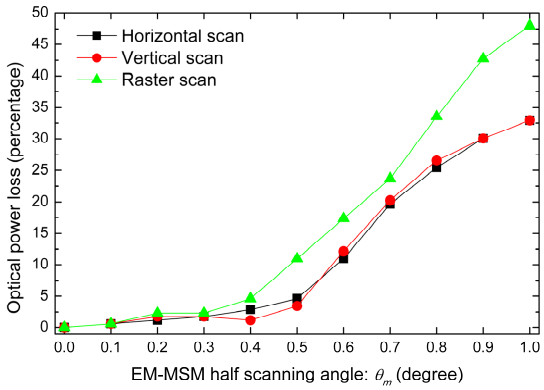

Fig. 4. The relationship between the EM-MSM half scanning angle θ_m and the optical power loss.

There are two factors that may cause the increment of optical power loss when the value of θ_m becomes large. Firstly, reflection at the uncoated entrance aperture of the MMF increases based on the Fresnel equation [26]; and secondly, the area of laser beam projected onto the entrance aperture plane of the MMF becomes larger, and hence the entrance aperture may collect fewer amount of lights.

4.2 Speckle reduction efficiency

Two conditions are experimentally carried out to quantitatively measure the speckle reduction efficiency, where the distance between the screen and the CCD camera Z_i and the F-number of the imaging lens $F\#_i$ are changed. In these situations, the imaging lens mounted on the CCD camera is adjusted to ensure it always focusing on the screen, and we have varied the gain value of the camera to keep the CCD sensors working in their linear region. Figures 5(a) and 5(b) show the speckle images when the EM-MSM is turned off or scans a raster trajectory at Z_i = 190 mm, $F\#_i$ = 2.1, and θ_m = 0.4 °, respectively; speckle images at Z_i = 900 mm and $F\#_i$ = 2.1 are shown in Figs. 5(c) and 5(d), where θ_m = 0 ° in Fig. 5(c) and θ_m = 0.4 ° in Fig. 5(d); Figs. 5(e) and 5(f) show the speckle images at Z_i = 900 mm and $F\#_i$ = 8 when θ_m = 0 ° and θ_m = 0.4 °, respectively. The speckle CRs under different EM-MSM half scanning angle θ_m are calculated and presented in Fig. 6. It is obvious that the MMF itself can reduce speckle where the speckle CRs are lower than 0.3 when the MSM is turned off; after the EM-MSM is driven, we can achieve further speckle reduction; more efficient speckle reductions are obtained by the raster scan comparing to the one-dimensional scans, and also by the increment of θ_m, *i.e.*, the increment of the half scanning angles by the EM-MSM. We can also find that when the value of $\theta_m \geq 0.4$ °, the speckle CR tends to saturate at about 0.194 for one-dimensional scans and at about 0.187 for raster scan when Z_i = 190 mm and $F\#_i$ = 2.1, while when Z_i = 900, it tends to saturate at about 0.152 and 0.084 for one-dimensional scans and at about 0.146 and 0.078 for raster scan at $F\#_i$ = 2.1 and $F\#_i$ = 8, respectively.

Optics EXPRESS

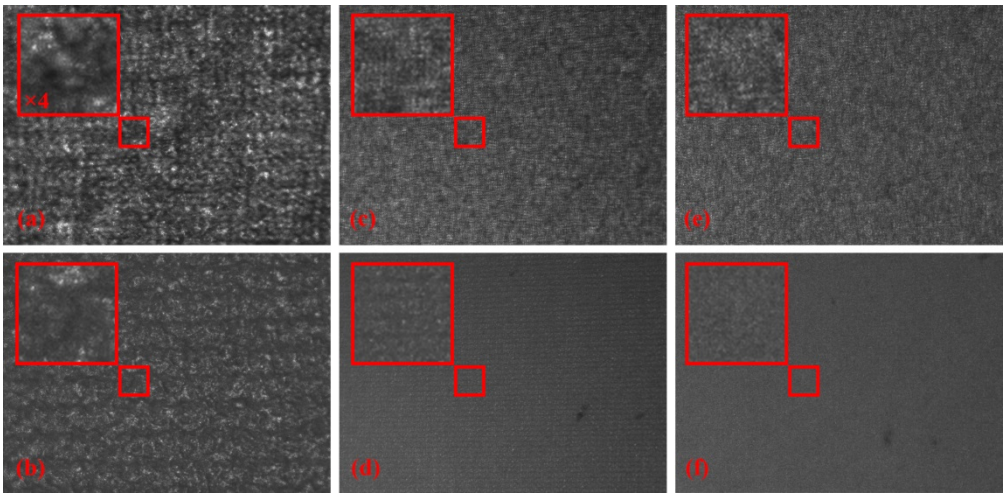

Fig. 5. Speckle images captured by the CCD camera at different distance between the screen and the CCD camera Z_i, F-number of the imaging lens $F\#_i$, and EM-MSM half scanning angle θ_m. (a) Z_i = 190 mm, $F\#_i$ = 2.1, and θ_m = 0 °, (b) Z_i = 190 mm, $F\#_i$ = 2.1, and θ_m = 0.4 °, (c) Z_i = 900 mm, $F\#_i$ = 2.1, and θ_m = 0 °, (d) Z_i = 900 mm, $F\#_i$ = 2.1, and θ_m = 0.4 °, (e) Z_i = 900 mm, $F\#_i$ = 8, and θ_m = 0 °, and (f) Z_i = 900 mm, $F\#_i$ = 8, and θ_m = 0.4 °.

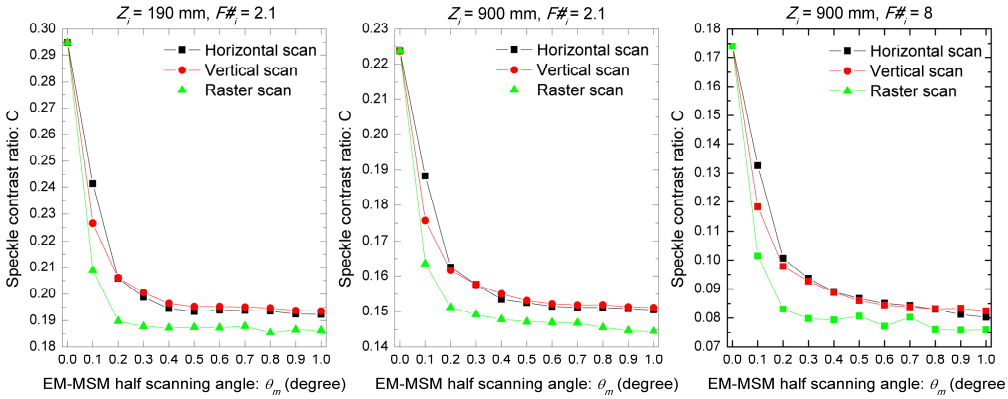

Fig. 6. Speckle CRs under different EM-MSM half scanning angle θ_m when the distances between the screen and the CCD camera Z_i and the F-number of the imaging lens $F\#_i$ are changed.

According to Eq. (2), the MMF has about $M = 3.1 \times 10^6$ modes. When raster scan instead of one-dimensional scans is introduced or when the value of θ_m increases, the phase modulation and mode coupling of the guided modes become more severe, and light distribution at the exit aperture of the MMF tends to be more random. Consequently, more different speckle images form on the screen during the integration time of the CCD camera; after the summation by the CCD camera, the speckle CR becomes lower.

The saturation trend of speckle CR when $\theta_m \geq 0.4$ ° shown in Fig. 6 can be explained by using the compound speckle theory and the Van Cittert-Zernike theorem [3]; these theories can also explain the phenomena for the same values of θ_m that the speckle CRs at Z_i = 190 mm are always larger than that at Z_i = 900 mm when $F\#_i$ = 2.1, and that the speckle CRs at $F\#_i$ = 2.1 are always larger than that at $F\#_i$ = 8 when Z_i = 900 mm. There are four speckle formation mechanisms in our experimental setup shown in Fig. 3, which are the random phase delays among the MMF modes, the scattering by the highly transparent diffuser, the interferences because of the total internal reflection of the tapered rod integrator, and the scattering on the screen. For simplicity purpose, we assume that the speckle forming on the

Optics EXPRESS

exit aperture of the tapered rod integrator resulting by the former three speckle formation mechanisms is the first speckle, and the speckle caused by the screen scattering is the second speckle; thus, the first speckle and the second speckles together compose the compound speckle on the screen. The compound speckle CR C after reduction can be written as [3]

$$C = \sqrt{\frac{T + S \pm 1}{N_o TS}}, \tag{6}$$

when the exit aperture of the MMF over fills (plus sign) or just fills (minus sign) the projection lens, where T and S represent the temporal degrees of speckle reduction freedom because of the scanning behavior of the MSM during the detector integration time, and the spatial degrees of speckle reduction freedom determined by the number of projection lens resolution elements lying within one imaging lens resolution spot, respectively; the factor of N_o represents the other individual degrees of speckle reduction freedoms such as the usage of the MMF and the independent orthogonal polarizations of the screen *etc*. In Eq. (6), the value of S can be simplified as the ratio between the solid angles of the projection lens and the diffraction-limited imaging lens [3]. Because the values of the solid angles are very small in our optical setup, S can be further simplified as [3, 16]

$$S \approx \left(\frac{Z_i F\#_i D_p}{f_i Z_p} \right)^2. \tag{7}$$

From Eq. (6), we can find that S is the dominate factor when $T >> S$, and the compound speckle CR C approaches to a constant value at $(N_o S)^{-1/2}$. This explains the saturation trend of speckle CR when $\theta_m \geq 0.4$ ° shown in Fig. 6, where the value of T become extreme large at these θ_m; According to Eq. (7), S is proportional to the squares of Z_i and $F\#_i$, and based on Eq. (6), C is inverse proportional to S. With the increment of the distance between the screen and the imaging lens from Z_i = 190 mm to Z_i = 900 mm at $F\#_i$ = 2.1, and with the increment of F-number of the imaging lens from $F\#_i$ = 2.1 to $F\#_i$ = 8 at Z_i = 900, the decreased compound speckle CRs agrees to the equations.

Considering the speckle perceived by human eyes, F-number $F\#_i$ and focal length f_i of the imaging lens should be set as

$$F\#_i = \sqrt{\frac{\pi A_{ccd}}{1.17\lambda^2}}, \tag{8}$$

$$f_i = \sqrt{\frac{D_{eye}{}^2 \pi A_{ccd}}{1.17\lambda^2}}, \tag{9}$$

where A_{ccd} and D_{eye} = 3.2 mm represent the area of one CCD sensor and the pupil diameter, respectively [27]. By substituting A_{ccd} = 27.04 μm^2 and λ = 520 nm used in our experiments to Eqs. (8) and (9), the F-number $F\#_i$ of and focal length f_i of the imaging lens are calculated as $F\#_i$ = 16.4 and f_i = 52.4 mm. According to Eq. (7), the value of S under this condition will be about 1.9 times higher than that when $F\#_i$ = 8 and f_i = 35 mm, which indicates the eyes will observe the speckle CR at about 0.057 instead of 0.078 measured by the CCD camera.

4.3 Potential applications in high lumen laser projectors

In high lumen laser projectors, many laser diodes are coupled into the corresponding MMFs to obtain the high power laser module [21, 22]. Though the speckle after driving the MSM can still be observed by the human eyes (human eyes can observe speckle when the speckle CR is equaling or higher than 0.05), in the future, we plan to fabricate a MSM array to modulate the laser diodes. Therefore, each laser diode illuminates the corresponding MSM

Optics EXPRESS

and MMF for speckle reduction, and the MMFs are assembled together to generate the high power laser module; by introducing different laser diodes with slight variations of their central wavelengths, and according to Eq. (1), the speckle CR can be reduced further [3]. For example, if there are thirty independent green laser diodes with enough central wavelength separations, an extra speckle reduction freedom equaling to thirty can be introduced, and the speckle CR can be reduced by an extra factor of $1/30^{1/2}$ [3, 5]. After compounding this extra speckle reduction mechanism with the EM-MSMs and the MMFs, the highest speckle CR equaling to 0.1873 presented in Fig. 6 by raster scan at θ_m = 0.4 ° can be further reduced to 0.0342, which is sufficient for speckle reduction considering the speckle CR detection level of the human eyes.

5. Conclusions

In conclusion, we have fabricated an EM-MSM and combined it with a MMF for laser speckle reduction. The speckle reduction efficiency is demonstrated, where by driving the EM-MSM in one-dimensional scans and raster scan, the compound speckle is reduced. We have discussed the optical power loss and the factors that affect the speckle reduction efficiency. The potential applications of this technique in high lumen laser projectors are also discussed. This technique is compact and can enable the integration of the high power laser module with reduced laser speckle for high lumen laser projection application. In the future, we plan to fabricate the electrostatic MSM to replace the EM-MSM, which can be produced in batch production and is more compact with lower power consumption.

Funding

National Key Research and Development Program of China (2016YFB0401903 and 2016YFB0402003); National Natural Science Foundation of China (NSFC) (61404104); Natural Science Foundation of Jiangsu Province (BK20140409); Changjiang Scholars and Innovative Research Team in University of Ministry of Education of China (IRT13076); State Key Program of National Natural Science of China (11434007).